Radio To X-ray Energy Emission Properties for [HB 89] Quasar's

M. N. Abdulhussein, L.M. Karim, H.H.Ali, U.A.Jallod
Department of Astronomy. College of Science, University of Baghdad. Baghdad-Iraq

Abstract

Statistical analysis were carried out for Active Galactic Nuclei (AGN) quasar's sample with low luminosity, selected from RBSC-NVSS catalogue of the brightest x-ray source emission down to optical and radio bands.

The x-ray in the (0.1 -2.4 keV band) properties are studied as a function of radio in 1.4 GHz (21 cm Hydrogen absorption line) and optical in (4400 Aº) fluxes for quasar's in this sample, having red shift ranges for $z > 1$ and $z < 1$.

Results showed a positive correlation between the X-ray and the radio luminosities (L_x-L_R),x-ray and optical luminosities (L_x-L_B). The slope of linear relations between (L_x-L_R) and (L_x-L_B) are flat (≤ 0.5), which indicates the existence of components unrelated with x-ray emission.

خواص طاقة الكوازرات [HB89] الانبعاثية للاطوال الموجية من الراديوية الى الاشعة السينية

الخلاصة

تحليلات احصائية استخرجت لعينة من النوى المجرية الفعالة(AGN) للكوازرات ذات النورانية الواطئة والتي تم استخراجها من كتالوك(RBSC-NVSS) لألمع المصادر ذات الحزم الانبعاثية السينية والمرئية والراديوية.

خواص الاشعة السينية ضمن الحزمة(0.1 -2.4 keV) تمت دراستها كدالة للفيض الراديوي 1.4 GHz (خط امتصاص الهيدروجين 21 cm) والفيض المرئي ضمن الطول الموجي في (4400A°) للكوازرات في هذه العينة ذات زحزحة حمراء ضمن المدى($1.0 < z < 1.0$) . اظهرت النتائج ان هناك علاقة ارتباط ايجابية بين النورانيات السينية والراديوية (L_x-L_R) وكذلك بين النورانيات السينية والمرئية (L_x-L_B) . العلاقات الخطية بين(L_x-L_R) و (L_x-L_B) كانت ذات ميل مسطح (≥ 0.5) ، والتي تشير الى وجود مركبات غير مرتبطة بالانبعاث السيني .

Introduction

Quasars are extremely luminous, extremely distant, active galaxies. Some are powerful radio sources, similar to the radio galaxies. Others are similar both to radio and Seyfert galaxies in that they are ejecting hot gas from their centers, as deduced from the extremely strong emission lines in their spectra [1].

A closer look at the continuous spectral of quasars that they actually have several separatel components. Over most of the spectrum of a quasar, the bulk of the continuous radiation is contributed by a feature less component that extends from the x-ray region to far infrared. This component is probably due to synchrotron radiation from energetic electrons moving through magnetic fields. For most quasars, the brightness of the synchrotron radiation fades rapidly with increasing wavelength in the radio part of the spectrum. In fact, most quasars are completely undetectable as radio sources, even though it was intense radio radiation that originally alerted astronomers to quasars [2].

Quasars are the most luminous objects in the universe and can thus be seen to highest red shift. Therefore, the represent ideal probes for testing directly the physical condition at large look back times. To do so, detailed knowledge is required about the mechanisms of the quasar

emission and about the cosmical evolution of the objects [3].

Comparison of global emission properties of galaxies at different wavelengths, from the radio to the x-rays can give us insight on the formation and evolution of galaxies, in particular, AGNs (Active Galactic Nuclei). For example, comparison of radio continuum and x-ray data of Seyfert galaxies or quasars with red shift range from $z > 1$ and $z < 1$ led to discovers a strong correlation between the radio and x-ray emission [4].

Moreover the comparison of global emission properties in a wide range of wavelengths can revel the relative importance of those components and processes responsible for observed association between global parameters of galaxies.

In this paper we report the statistical analysis of the sample of AGNs selected from RBSC-NVSS sample of the brightest x-ray sources. The sample is large enough for detail study of multi-frequency properties of AGNs [5].

We generally collected all quasars (quasi-star object,QSO) for $z > 1$ and $z < 1$ which a published radio, optical and x-rays fluxes can be obtained from RBSC-NVSS sample. In the next section we will present the data and give details of the derivation of the relevant parameters.

Correlation between radio, optical and x-ray luminosities (L_R, L_B and L_X) have been demonstrated in quasars. The form and strength of the correlation may reveal information about the energetic and sources of emission.

The sample, data and derived parameters

The ROSAT all-sky survey covers 92% of entire in the soft (0.1-2.4 kev) X-ray, with counts s^{-1} ($\sim 10^{12}$ erg.s^{-1}.cm^{-1}) completeness limit.

Bauer et al [5] have cross-identified the ROSAT Bright Source Catalogue (RBSC) and the National. Radio Astronomy Observatory (NRAO), together with Very Large Antenna (VLA) Sky Survey (NVSS) to construct [RBSC-NVSS] sample of the brightest x-ray sources that are also radio sources($S \geq 2.5$ mJy at 1.4GHz).

In [RBSC-NVSS] sample besides x-ray and radio data the blue magnitudes (m_B), red shift (z) and AGN types (quasars) are presented too. Therefore, for statistical investigation of multi-frequency properties of AGN, specifically Quasars (QSO), the RBSC-NVSS sample gives exception opportunity for detail study.

The relation between the observed flux and the luminosity is given by Schmidt and Green [6] as:

$$L(E1, E2) = 4\pi * C(z) * A^2(z) * f(E1, E2) \quad \ldots\ldots\ldots (1)$$

Where E1 to E2 are every band, where C (z) is the K-correction term, A (z) is the luminosity distance term, f (E1, E2) observed flux density, and (z) is the red shift.

For power-law spectra with energy index (α) and Friedmann cosmology with Hubble constant H_o = 75 Km s^{-1} Mpc^{-1} = ($24.3058*10^{-19}$ sec^{-1}) and deceleration parameter q_o=0.5, the luminosity distance term A(z) and the K-correction term C(z) are given by:

$$A(z) = 2(c/H_o)\,[(1+z)-(1+z)^{0.5}] \quad \ldots\ldots\ldots\ldots (2)$$

Where (c) is the velocity of light.

$$C(z) = (1+z)^{-(1+\alpha)} \quad \ldots\ldots\ldots\ldots (3)$$

Which after substitution equation (2) and (3) in equation (1), yields to

$$L(E1,E2) = 4\pi * (c/H_o)^2 * (1+z)^{-(1+\alpha)}\,[2*((1+z)-(1+z)^{0.5})]^2 * f(E1,E2) \quad \ldots\ldots\ldots (4)$$

Which is the general equation of the luminosity as a function of energies.

The monochromatic fluxes in the optical band at 0.44 μm (4400A˚) are calculated by [7]

$$F_{opt}(4400A^{\circ}) = 10^{(-0.4\, m_B - 19.344)}\ [\text{erg cm}^{-2}\ \text{s}^{-1}\ \text{Hz}^{-1}] \quad \ldots (5)$$

The calculated luminosities in the x-ray (0.1 - 2.4keV) band, in the radio band of (1.4 GHz) and optical band at (4400A˚) are referred to as L_x,L_R and L_B respectively, and are given in (erg s^{-1}) or (erg s^{-1} Hz^{-1}). The energy indices for quasar's continuum are equal :

α = -1.02 for x-ray band [3]

α= -0.5 for optical band , and α = -0.8 for radio band [8] .

Luminosity correlations and results

For each sample of AGN galaxies we have calculated all correlation coefficients from radio to x-ray bands, including distance parameter (red -shift) in order to reduce Malmquist bias (distance dependence. selection effect) on the estimates of correlation coefficients and enlarge the number of galaxies for each sub-sample. Accordingly improving the results of statistics,

the missing observational data at any wavelength have been substituted by mean of the corresponding variable. As a result, this procedure significantly reduces artificial correlations between luminosities and distance, caused by the fact that at large distance we observe the more powerful sources. Then we selected only those pairs of variables, which showed significant correlations ($p<0.01$). Then we have performed multiple regression analysis to learn more about the relationship between variables involved [9].

In general, multiple regression procedure will estimate a linear equation of the form:

$$Y= a+b_1x_1+b_2 x_2 +\ldots\ldots+b_nx_n \quad \ldots\ldots (6)$$

Where Y is dependent variable (Log L_x), $x_1, x_2, \ldots x_n$ are independent variables (Log L_R, Log L_B, …, Log L_n) respectively, (a) is the intercept value, and $b_1, b_2, \ldots b_n$ are the slopes as the regression coefficients.

Note that in this equation, the regression coefficients represent variable to the prediction of each variable. This type of correlation is also referred to as a partial correlation. We have applied this technique for the of [HB 89] Quasars samples:

a) For [HB 89] Quasar's type 1, with ($z<1.0$): Log L_x= (0.46±0.24) Log L_R+ (0.43±0.24) Log L_B+ (-14.11±24.08)

Log L_x N=14	Log L_R	Log L_B
	$r_{1.4}$=0.44 ; $P_{1.4}$=0.0713	r_B=0.41; P_B =0.095

Where $r_{1.4}$, r_B, $P_{1.4}$, P_B are correlation coefficients and significance level (Probability of chance correlation) respectivly, and(N) represent the number of [HB 89] Quasar's used in the sample.

b) For [HB 89] Quasar's type 2, with ($z.>1.0$): Log L_x= (0.29±0.15) Log L_B + (29.21±5.69)

Log L_x N=43	Log L_B
	r_B=0.36 ; P_B =0.059

c) For [HB 89] Quasar's combination of type 1 and 2.

Log L_x=(0.51±0.11) Log L_R+(.021±0.11) Log L_B + (15.87±7.43).

Log L_x N=57	Log L_R	Log L_B
	$r_{1.4}$=0.56 ; $P_{1.4}\approx10^{-5}$	r_B=0.35 ; P_B =0.058

The results of multiple regression analysis show apparently that the x-ray emission of AGN (Quasar's HB 89) is correlated with the radio and optical emission. Moreover, the slopes of the correlations between the x-ray and optical emission for [HB 89] Quasar's types (1) are significantly steeper than for [HB89] Quasar's type (2) and type (1, 2) with (P=0.095). The lack of correlation between x-ray and radio luminosities for [HB 89] Quasar's type (2) perhaps indicates that association of x-ray emission with blue continuum is more fundamental and possible weak correlation between x-ray and radio emission may disappear from multiple regression analysis, because of tight correlation between the x-ray and optical emission. The joint dependence of x-ray on optical and radio luminosity for [HB 89] Quasar's type 1 and 2 is strikingly similar to that which was found for quasar's [10], although different statistical techniques have been used.

Discussion and conclusions

The principal result of our study, presented in section 3, is the existence of a good correlation between x-ray (0.1-2.4 keV), radio (1.4GHz in 21 cm) and optical (4400A°) luminosities. The above correlations that the x-ray, optical and radio emission are physically connected. The impressive fundamental correlation between the x-ray, optical and radio emission over many decays (see figures 1 to 5) of both luminosities indicates on similar origin for the radiation of all AGNs(e.g. Quasar's). The [HB 89] Quasar's in this sample show different slopes in relation between L_x-L_R and L_x-L_B , a fact that can not be accommodate easily in orientation-related unification schemes. Figure (3) shows the correlation of the x-ray luminosity with the monochromatic (4400A°) optical luminosity. Very similar slopes for the L_x-L_B relation have been found for x-ray selected sample of RBSC-NVSS. This seems to indicate that the high emission in quasars is of similar origin, independent of the quasar's radio properties.

In the luminosity-luminosity scatter diagrams we find positive correlation between the x-ray luminosity and optical and radio luminosities, respectively, are shown in the figures.

In the L_x-L_R relation, the x-ray emission in quasar's is commonly interpreted as originating

in AGN. The coronal x-ray cooling is mostly generated through computerization of the softer photospheric disk photons, rather than through pure thermal emission . This variability pattern is interpreted as magnetic reconnection event in the corona, which accelerates electrons , producing a synchrotron emission spike, the high energy electron beam dumpes its energy collisionally in the cooler chromospheric gas, heating it to coronal temperature, and thus raising the coronal x-ray emission. Radio and x-ray monitoring of quasar's may thus provide further evidence for the coronal origin of the radio emission occure in QSOs, and may thus shed some light on the coronal heating process in AGN.

We may conclude that the investigation of multi-wavelength radio to x-ray properties of AGNs (HB 89Quasar's) led us to the following points :

(a) The positive correlation between x-ray, optical and radio emission over many decades is primary and it indicates on intrinsically similar origin of both radiations in quasar's, powered mainly by AGN, rather than compact starbursts, For [HB 89] Quasar's we found that the slopes of relation L_X-L_R and L_x-L_B are flat (≤ 0.5) which indicate on existence of components unrelated with x-ray.

(b) Coronally active stars also show a tight relation between L_X and L_R, which together with correlated variability indicates that stellar corona are magnetically heated.

(c) Distance (red shift) biases (chiefly the Malmquist bias) are a well known danger in any correlation analysis, and may result in spurious luminosity correlations when working with flux limited sample. Our results directly confirm that a Malmquist bias is not significant.

Most regression bisector slopes (see figure 1-5) indicate non-Linear relationship between variables (Flat slopes). If the correlation were due to a Malmquist bias, they would only appear as linear relationship in the log-log plane (power-law=1).

Table 1: Data analysis for [HB 89] Quasar's type 1 ((Z >1.0)

No.	Name	F_x ($erg.s^{-1}.cm^{-2}$)	$F_{1.4}$ (mJy)	m_B	Z	F_{opt} ($erg.s^{-1}.cm^{-2}.Hz^{-1}$)	Log L_x (erg/s)	Log L_R ((erg/s.Hz)	Log L_B (erg/s.Hz)
1	0035-252	2.04	412.9	17.5	1.196	4.52898E-27	45.90767	34.13873	31.07639
2	0232-042	2.36	1495.9	16.5	1.45	1.13763E-26	46.15802	34.87439	31.63874
3	0402-362	2.07	1151.1	17.2	1.417	5.97035E-27	46.07866	34.73948	31.33939
4	0435-300	2.22	1091.4	17.5	1.328	4.52898E-27	46.04596	34.65686	31.16478
5	0440-285	2.72	357.1	19.2	1.952	9.46237E-28	46.51018	34.52498	30.80715
6	0448-392	1.63	542.7	16.5	1.288	1.13763E-26	45.88209	34.32538	31.53899
7	0903+198	2.57	16.8	16.4	1.206	1.24738E-26	46.01604	32.75582	31.52343
8	1055+201	2.06	350.6	17.1	1.11	6.54636E-27	45.83971	33.99932	31.17322
9	1416+067	5.62	6100.8	16.8	1.436	8.62979E-27	46.5254	35.47598	31.51059
10	1411+522	5.12	2543.9	20	1.57	4.52898E-28	46.57189	35.17794	30.30546
11	2008-159	4.1	546.5	17.2	1.18	5.97035E-27	46.19778	34.24813	31.185
12	2126-158	3.50	590.1	17.3	3.268	5.44503E-27	50.06625	35.21423	31.99024
13	2149-307	7.17	1243.6	18.4	2.345	1.97697E-27	47.11112	35.23492	31.27892
14	2223+210	3.52	1837.6	18.2	1.959	2.37684E-27	46.62567	35.23972	31.21013

Table 2: Data analysis for [HB 89] Quasar's type2 (Z < 1.0)

No.	Name	F_x ($erg.s^{-1}.cm^{-2}$)	$F_{1.4}$ (mJy)	m_B	Z	F_{opt} ($erg.s^{-1}.cm^{-2}.Hz^{-1}$))	Log L_x (erg/s)	Log L_R (erg/s.Hz)	Log L_B (erg/s.Hz)
1	0017+257	3.94	684.3	15.4	0.284	3.13329E-26	44.83851	33.05438	31.53276
2	0133+207	5.11	3901.9	18.1	0.425	2.60615E-27	45.3234	34.17242	30.76048
3	0135-247	2.09	1181.9	17.3	0.831	5.44503E-27	45.56767	34.26232	31.56477
4	0137+012	3.23	131106	17.1	0.26	6.54636E-27	44.67151	35.25785	30.78385
5	0137-010	5.17	3.3	16.5	0.334	1.13763E-26	45.10543	30.88292	31.21795
6	0214+108	8.95	1376.2	17	0.408	7.17794E-27	45.52886	33.68303	31.16986
7	0231+022	4.05	52.1	18	0.321	2.85759E-27	44.96285	32.04564	30.58747
8	0340-372	1.69	2060.4	18.6	0.284	1.64437E-27	44.4709	33.53308	30.25276
9	0346-279	1.36	840	19.4	0.988	7.87046E-28	45.5471	34.27218	30.84405
10	0349-146	2.38	3045.1	16.2	0.6163	1.49968E-26	45.33997	34.40112	31.79329
11	0414-060	3.24	766.7	15.9	0.775	1.97697E-26	45.69145	34.0107	32.07603
12	0454-220	4.05	1991.4	16.1	0.5335	1.64437E-26	45.43495	34.0858	31.72868
13	0812+020	4.1	1755.9	17.1	0.402	6.54636E-27	45.17607	33.7755	31.11872
14	0833+446	9.07	7.1	15.6	0.255	2.60615E-26	45.1022	30.97415	31.36863
15	0837-120	0.12	1863.7	15.8	0.1976	2.1677E-26	42.99221	33.16618	31.08659
16	0903+169	3.82	1587.1	18.3	0.4121	2.1677E-27	45.16839	33.75396	30.65737
17	0911+053	2.87	456	17.4	0.303	4.96592E-27	44.76026	32.93605	30.78297
18	0937+391	1.56	689.1	17.5	0.618	4.52898E-27	45.15912	33.7583	31.27527
19	0952+457	1.45	57.4	16.7	0.259	9.46237E-27	44.32016	31.8957	30.94083
20	1007+303	2.09	2.9	17	0.26	7.17794E-27	44.48246	30.60263	30.82385
21	1007+417	2.97	499	16.5	0.6123	1.13763E-26	45.43	33.6097	31.6686
22	1011-282	3.64	8.33	16.9	0.253	7.87046E-27	44.69852	31.03651	30.84245
23	1040+011	6.28	33.2	19.2	0.73	9.46237E-28	45.92188	32.59269	30.71394
24	1049+616	3.35	988.9	16.5	0.422	1.13763E-26	45.13344	33.56991	31.39518
25	1111+149	1.48	642.3	18	0.869	2.85759E-27	45.46058	34.03831	31.3158
26	1128+315	9.62	370.4	16.6	0.289	1.03753E-26	45.24217	32.80341	31.06632
27	1200-051	5.56	530.5	18	0.381	2.85759E-27	45.25862	33.20739	30.71822
28	1208+322	1.37	370.4	16	0.388	1.80302E-26	44.66713	33.06776	31.53199
29	1217+023	4.77	673.7	16.5	0.24	1.13763E-26	44.76788	32.89728	30.96095
30	1219+044	1.45	800.8	18	0.965	2.85759E-27	45.55226	34.22988	31.38795
31	1223+252	2.11	365.4	16	0.268	1.80302E-26	44.51426	32.73006	31.24756
32	1351+267	2.77	246.2	17.2	0.31	5.97035E-27	44.76583	32.68884	30.88061

33	1352-104	3.67	768.7	18.4	0.332	1.97697E-27	44.95108	33.24478	30.45334
34	1354+195	1.78	2586.3	16	0.72	1.80302E-26	45.36122	34.47166	31.9842
35	1457-375	8.47	942.7	16.7	0.314	9.46237E-27	45.26301	33.28341	31.09049
36	2310-322	4.66	817.4	16.6	0.337	1.03753E-26	45.06857	33.28487	31.1848
37	2340-036	4.44	361.5	16	0.896	1.80302E-26	45.96703	33.81663	32.13695
38	2352-342	1.61	331.4	16.4	0.706	1.24738E-26	45.29896	33.56145	31.8103
39	1522+113	3.43	408.1	18	0.331	2.85759E-27	44.91893	32.96708	30.61103
40	1716+686	3.21	489.3	18.5	0.777	1.80302E-27	45.68986	33.818	31.03784
41	1721+343n	0.217	1614.1	16.5	0.206	1.13763E-26	43.28716	33.14074	30.83984
42	2140-048	3.26	806.1	18	0.344	2.85759E-27	44.93235	33.29728	30.64053
43	2227-399	6.34	584.1	18.5	0.323	1.80302E-27	45.1632	33.10086	30.39224

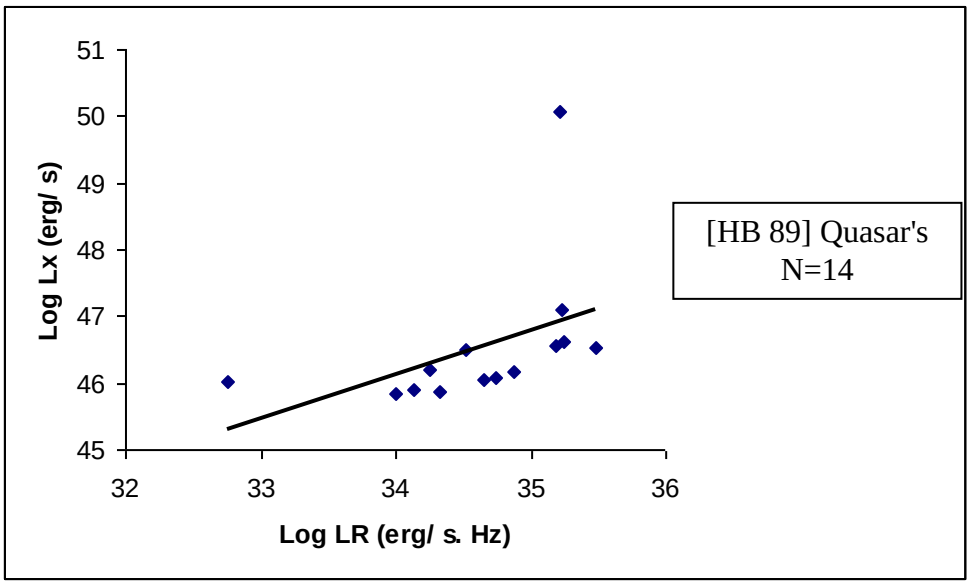

Fig 1 : X-ray luminosity (L_x) as a function of radio luminosity (L_R),denoted by (•) for [HB 89] Quasar's type 1 (Z > 1.0). The solid line represent the linear regression.

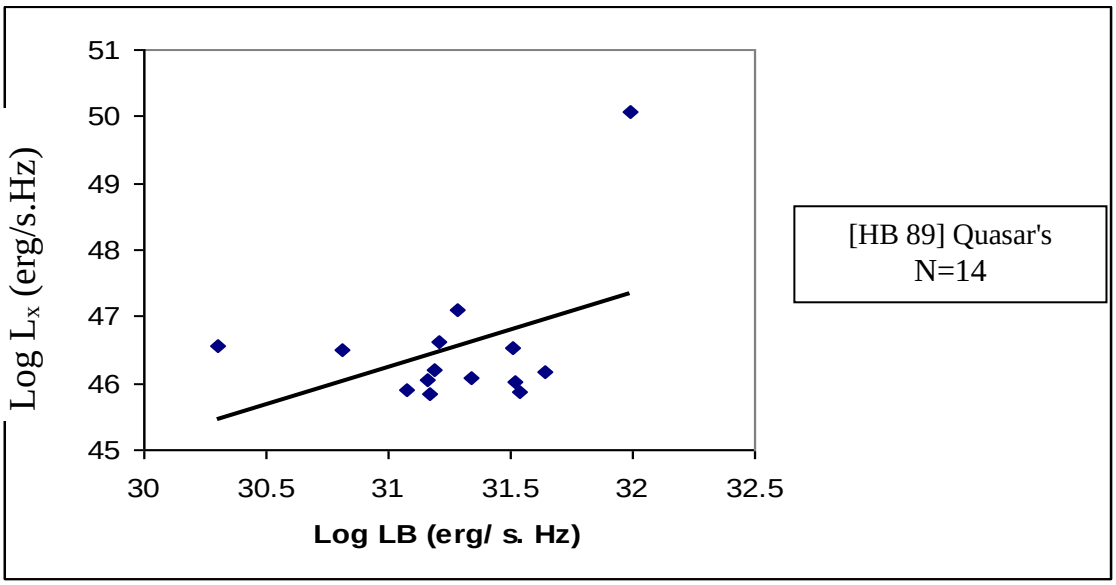

Fig 2: X-ray luminosity (L_x) as a function of optical luminosity (L_B) for [HB 89] Quasar's type 1 (Z > 1.0)

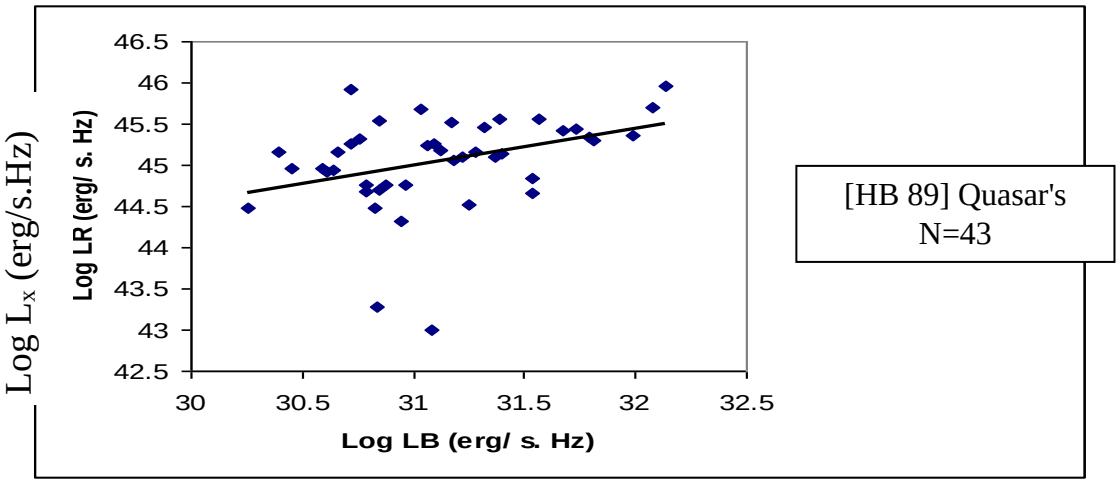

Fig 3 : X-ray luminosity (L_x) as a function of optical luminosity (L_B) for [HB 89] Quasar's type 2 (Z < 1.0).

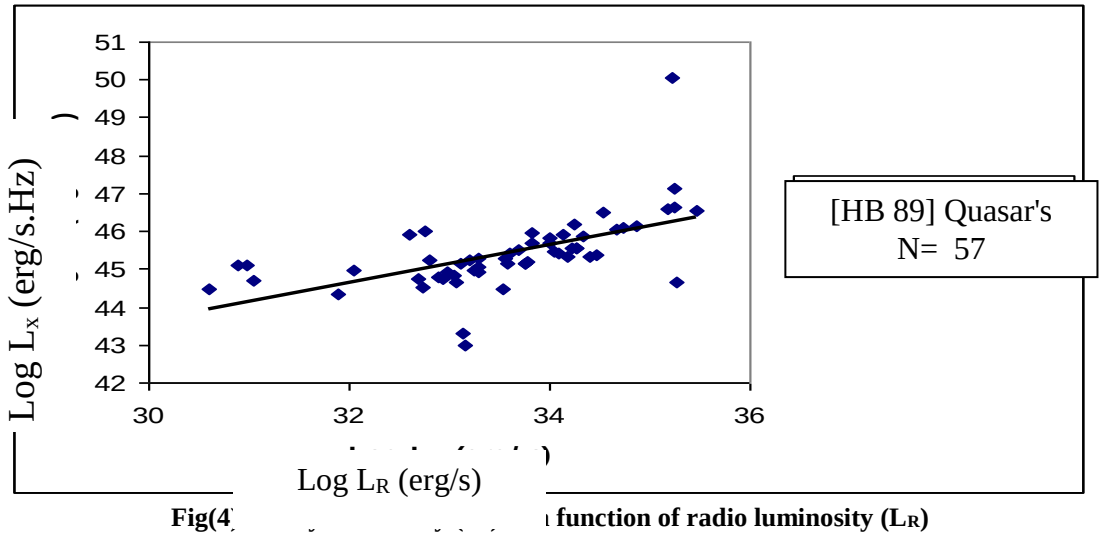

Fig(4) function of radio luminosity (L_R) for [HB 89] Quasar's type (1 and 2) .

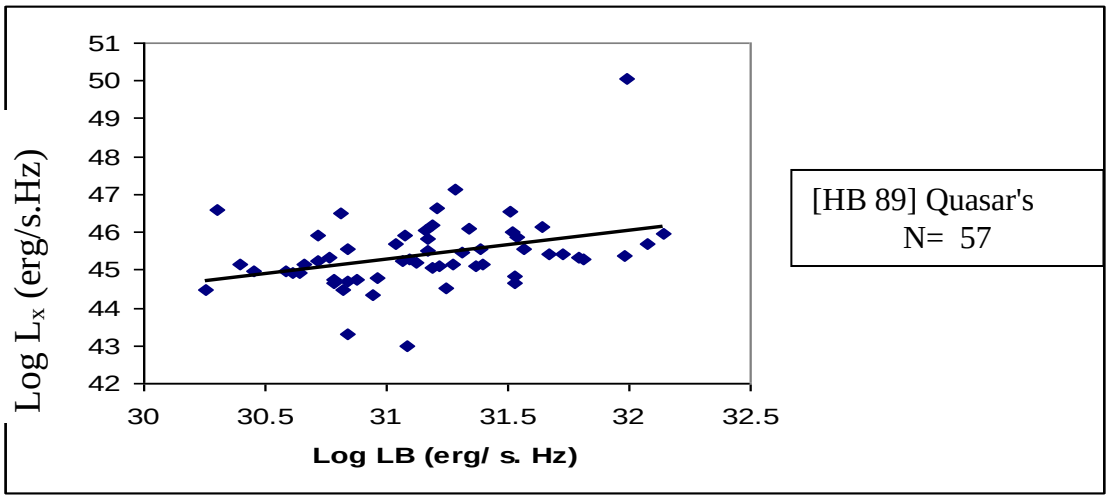

Fig 5: X-ray luminosity (L_x) as a function of optical luminosity (L_B) for [HB 89] Quasar's type (1 and 2).

References

1. Thomas T.Arny, **1998**. "*Explorations, An introduction to Astronomy*" ,second edition, WCB/MCGraw-Hill,
2. John. D. Fix, **1995**. "*Astronomy, Journey to the cosmic frontier*", Mosby-Year book, Inc., first edition.
3. W.brinkmann, W.yuan and J. siebert , **1997**."*broad band energy distribution of ROSAT detected quasars*", Astron. Astrophys. 319, 413,.
4. R.A. Kandalyan,**1987**. "Three-Dimensional Luminosity Function of Type 1 Seyfert Galaxies", Astrophysics,26,301. , 45, 277.
5. Bauer, J. J. Condon, T.X. Thuan, J.J. Broderick, **2000**, "*RBSC-NVSS Sample I. Radio and Optical Identifications of A Complete Sample of 1500 Bright X-Ray Sources*". Astrophys. J., Supple. Ser., 129, 547,.
6. M. Schmidt, R. F. Green, **1986**."*Counts, Evolution, And Back Ground Contribution Of X-ray Quasars And Other Extra Galactic X-ray Source*",Astrophys. J., 305, 68,.
7. Th. Boller, E., J., A., Meurs, W Brinkmann H.fink, U.Zimmermann, and H., M., Adrof,**1992.**,"Rosat *All Sky Survey Observation Of Iras Galaxies*", A stro. Astrophys. , 261,57,.
8. C.R. Canizares, J.L.White, **1989**," The X-Ray Spectra of High-Redshift Quasars",Astrophs. J.,339,27.
9. A. T. Kalloghlian, R. A. Kandalyan, H. M. K. Al-naimiy, A. M. Khassawneh, Astrophysics, 44, 359, **2001**."*Investigation of Barred Galaxies. v11. A comparative statistics of SB And SA Galaxies. Near IR Region*"
10. D.M. Worral, H.Tananbaum, P.Giommi and G.Zamorani, **1987.**"*x-ray studies of quasar's with Einstein observatory. Iv-x-ray defendence on radio emission*", Astrophs.J., 313,596.